J Comput Aided Mol Des
DOI 10.1007/s10822-006-9059-x

ORIGINAL PAPER

# Do benzodiazepines mimic reverse-turn structures?

**Masayuki Hata · Garland R. Marshall**

Received: 10 April 2006 / Accepted: 22 July 2006


**Abstract** The role of benzodiazepine derivatives (BZD) as a privileged scaffold that mimics $\beta$-turn structures (Ripka et al. (1993) Tetrahedron 49:3593–3608) in peptide/protein recognition was reexamined in detail. Stable BZD ring conformers were determined with MM3, and experimental reverse-turn structures were extracted from the basis set of protein crystal structures previously defined by Ripka et al. Ideal $\beta$-turns were also modeled and similarly compared with BZD conformers. Huge numbers of conformers were generated by systematically scanning the torsional degrees of freedom for BZDs, as well as those of ideal $\beta$-turns for comparison. Using these structures, conformers of BZDs were fit to experimental structures as suggested by Ripka et al., or modeled classical $\beta$-turn conformers, and the root-mean-square deviation (RMSD) values were calculated for each pairwise comparison. Pairs of conformers with the smallest RMSD values for overlap of the four $\alpha$–$\beta$ side-chain orientations were selected. All overlaps of BZD conformers with experimental $\beta$-turns yielded one or more comparisons where the least RMSD was significantly small, 0.48–0.86 Å, as previously suggested. Utilizing a different methodology, the overall conclusion that benzodiazepines could serve as reverse-turn mimetics of Ripka et al. is justified. The least RMSD values for the overlap of BZDs and modeled classical $\beta$-turns were also less than 1 Å. When comparing BZDs with experimental or classical $\beta$-turns, the set of experimental $\beta$-turns selected by Ripka et al. fit the BZD scaffolds better than modeled classical $\beta$-turns; however, all the experimental $\beta$-turns did not fit a particular BZD scaffold better. A single BZD ring conformation, and/or chiral orientation, can mimic some, but not all, of the experimental $\beta$-turn structures. BZD has two central ring conformations and one chiral center that explains why the four variations of the BZD scaffold can mimic all types of $\beta$-turn structure examined. It was found, moreover, that the BZD scaffold also mimics each of the nine clusters of experimental orientations of side chains of reverse turns in the Protein Data Bank, when the new classification scheme for the four side-chain directions (the relative orientations of $\alpha$–$\beta$ vectors of residues i through i+3) was considered (Tran et al. (2005) J Comput-Aided Mol Des 19:551–566).

**Keywords** Reverse turn · Beta-turn · Benzodiazepine · Privileged scaffold · Peptidomimetic · Conformational mimicry · Systematic search

## Introduction

A $\beta$-turn is a secondary structure element of peptide/proteins that consists of four residues (i, i+1, i+2 and i+3) that show peptide-chain reversal [1]. This turn may, or may not, be stabilized by internal hydrogen bonding between the carbonyl oxygen of residue i and the N–H of residue i+3. Several classic types of $\beta$-turn have been characterized by their $\phi_{i+1}$, $\Psi_{i+1}$, $\phi_{i+2}$ and $\Psi_{i+2}$ torsion angles (Table 1). Unfortunately, the

**Electronic Supplementary Material** Supplementary material is available to authorised users in the online version of this article at http://dx.doi.org/10.1007/s10822-006-9059-y.

M. Hata · G. R. Marshall (✉)
Center for Computational Biology, Washington University School of Medicine, 700 S. Euclid Ave., St. Louis, MO 63110, USA
e-mail: garland@pcg.wustl.edu

**Table 1** $\phi$ and $\Psi$ angles (degree) of residues i+1 and i+2 and $C_{\alpha I}$–$C_{\alpha i+1}$–$C_{\alpha i+2}$–$C_{\alpha i+3}$ angles (degree) in the representative experimental $\beta$-turns and ideal $\beta$-turns used in this study

| Structure | $\phi_{i+1}$ | $\Psi_{i+1}$ | $\phi_{i+2}$ | $\Psi_{i+2}$ | $\theta^a$ |
|---|---|---|---|---|---|
| *Type I* | | | | | |
| 1SBT (Gly23-Val26) | –52.3 | –58.2 | –90.8 | 22.0 | 34.6 |
| Ideal turn | –60.0 | –30.0 | –90.0 | 0.0 | 47.3 |
| *Type I′* | | | | | |
| 1STN (Ala94-Lys97) | 50.5 | 47.8 | 76.5 | –3.0 | –48.6 |
| 2SNM (Ala94-Lys97) | 46.3 | 51.6 | 71.0 | 4.7 | –50.4 |
| 2SNS (Ala94-Lys97) | 66.1 | 30.6 | 82.0 | 7.5 | –51.8 |
| Ideal turn | 60.0 | 30.0 | 90.0 | 0.0 | –47.3 |
| *Type II* | | | | | |
| 132L (Cys115-Thr118) | –53.7 | 129.4 | 94.9 | –7.0 | 25.7 |
| 1LMA (Cys115-Thr118) | –52.3 | 123.2 | 78.8 | –0.6 | 3.3 |
| 7LYZ (Cys115-Thr118) | –40.8 | 118.8 | 62.6 | 39.5 | –3.5 |
| Ideal turn | –60.0 | 120.0 | 80.0 | 0.0 | 2.4 |
| *Type II′* | | | | | |
| 1CBX (Tyr277-Leu280) | 63.1 | –115.7 | –82.2 | –16.8 | –3.2 |
| 1CPS (Tyr277-Leu280) | 67.2 | –134.5 | –69.4 | –15.4 | –7.5 |
| 4CPA (Tyr277-Leu280) | 42.5 | –122.4 | –68.9 | –13.4 | 8.4 |
| 6CPA (Tyr277-Leu280) | 68.2 | –132.5 | –72.6 | –16.6 | –6.3 |
| Ideal turn | 60.0 | –120.0 | –80.0 | 0.0 | –2.4 |
| *Type III* | | | | | |
| 1MBC (Phe46-Leu49) | –56.4 | –22.5 | –72.7 | –25.3 | 65.1 |
| 2CMM (Phe46-Leu49) | –56.9 | –22.2 | –86.1 | –1.7 | 55.5 |
| 2MGL (Phe46-Leu49) | –18.3 | –55.8 | –64.3 | –16.6 | 57.6 |
| Ideal turn | –60.0 | –30.0 | –60.0 | –30.0 | 67.2 |
| *Type IV* | | | | | |
| 1ACB (Ile99-Asp102) | –104.2 | 154.1 | 56.6 | 47.4 | 18.6 |
| 1CHO (Ile99-Asp102) | –87.4 | 147.3 | 61.4 | 48.9 | 20.5 |
| 5CHAb (Ile99-Asp102)[b] | -82.1 | 153.0 | 63.2 | 51.6 | 24.1 |
| *Type VI* | | | | | |
| 1RBD (Lys91-Asn94) | –53.2 | 136.1 | –79.7 | –8.3 | 33.3 |
| 1RBF (Lys91-Asn94) | –58.7 | 135.3 | –86.6 | –4.6 | 28.5 |
| 1RBG (Lys91-Asn94) | –54.0 | 138.0 | –81.8 | –4.1 | 24.2 |
| 1RNV (Lys91-Asn94) | –58.7 | 135.9 | –81.4 | –7.2 | 27.4 |
| Ideal turn[c] | –60.0 | 120.0 | –90.0 | 0.0 | –3.1 |

[a] $C_{\alpha I}$–$C_{\alpha i+1}$–$C_{\alpha i+2}$–$C_{\alpha i+3}$ angle of the peptide

[b] Structure B of 5CHA

[c] Type VIa1

relative orientation of the side chains of residues i and i+3 are not determined as the torsional angles $\Phi_i$ and $\Psi_{i+3}$ are not designated for classical $\beta$-turns.

$\beta$-Turns are recognition sites of peptides and proteins. Examples are found in high-resolution crystal structures of antibody-peptide complexes [2–4] and from structure-activity studies of many peptide hormones: i.e., angiotensin II [5, 6], bradykinin [7], gonadotrophin releasing hormone [8–10], somatostatin [11, 12], etc. Therefore, mimicking the three-dimensional recognition features of $\beta$-turns to generate peptidomimetics is important for developing agonists or antagonists of these molecular-recognition sites in biological systems.

Peptidomimetics have been generically classified into three types [13]. A type-I mimetic focuses on peptide-backbone mimicry. A type-II mimetic is simply a functional mimetic that does not necessarily mimic the chemical and/or topological structure of the parent peptide. The mode of binding to the receptor is different from that used by the parent peptide. A type-III mimetic is a topographical mimetic that contains the necessary functional groups positioned on a novel non-peptide scaffold to interact in a similar, if not identical, manner with the receptor. In current jargon, it presents the same three-dimensional pharmacophore necessary for recognition as the parent peptide. Some examples thought to be type-III $\beta$-turn mimetic [14] are found in the literature based on sugar rings [15, 16], pentaazacrowns [17], steroids [18], or heterocycles [19, 20].

Benzodiazepine (BZD) is one class of compounds postulated as a type-III $\beta$-turn peptidomimetic [13] that has a prototypical privileged substructure [21, 22]. Derivatives of this compound bind not only to BZD receptors of the central nervous system, but also to cholecystokinin receptors [21, 23]. Moreover, BZD compounds also act as Ras farnesyltransferase

inhibitors, HIV tat antagonists, reverse transcriptase inhibitors, κ-selective opioid antagonists, platelet activation factor antagonists or glycoprotein IIb/IIIa inhibitors [24, 25]. BZDs may demonstrate such widespread biological activities because the BZD central ring structure is a priviledged structure that can orient substituents to mimic the side-chain orientations of peptide reverse-turn structures, a common recognition motif in biological systems.

To examine this hypothesis, comparison of BZDs to β-turns was reexamined in detail in this study. Previously, Ripka et al. modeled BZDs as β-turn peptidomimetics and compared them with several kinds of experimentally determined structures of β-turns [26]. Figure 1 shows the schematic chemical structures of BZD and a β-turn. When Ripka et al. fit the four C–C vectors (a–b, c–d, e–f and g–h) of BZD to corresponding $C_\alpha$–$C_\beta$ vectors (a′–b′, c′–d′, e′–f′ and g′–h′) of β-turns (Types I, I′, II, II′, III, IV and VI), overlaps of the four vectors with less than 1 Å root-mean-square deviation (RMSD) values were obtained for some of the pairwise comparisons of each turn conformation selected. For this reason, they argued the BZD nucleus was an excellent potential mimic of each of the β-turn types. The methodology utilized (which we now assume to be constrained minimization) was not detailed in the literature leading to initial difficulties in reproducing the results. Ripka et al. [26] selected a basis set of proteins (Table 2) for comparison of

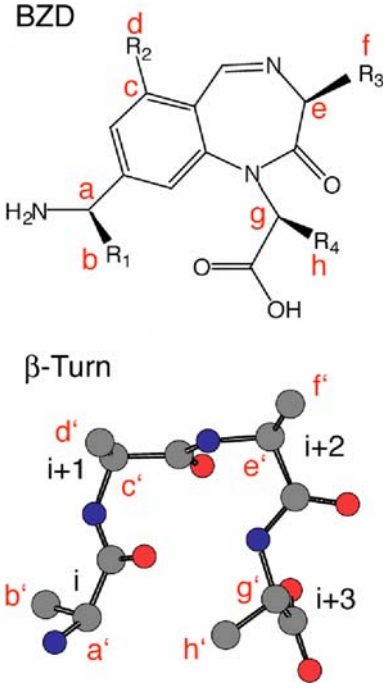


**Fig. 1** BZD and β-turn structures

**Table 2** Basis set of experimental β-turns used in both this study and that of Ripka et al.

| Type | Protein | Sequence (residue number) |
|---|---|---|
| Type I | Subtilisin BPN′ | GSNV (23–26) |
| Type I′ | Staphylococcal nuclease | ADGK (94–97) |
| Type II | Hen egg white lysozyme | CKGT (115–118) |
| Type II′ | Carboxypeptidase A | YGFL (277–280) |
| Type III | Sperm whale myoglobin | FKHL (46–49) |
| Type IV | α-Chymotrypsin | INND (99–102) |
| Type VI | Bovine ribonuclease S | KYPN (91–94) |

β-turns, but failed to indicate the Protein Data Bank (PDB) [27] accession number for the crystal structures used. The BZD structure utilized for comparison was derived with molecular mechanics (MM) calculations, but the resulting BZD coordinates were not included in the paper.

Due to the growing number of examples of BZDs as peptidomimetics and the probable importance of benzodiazepines as privileged scaffolds and type III peptidomimetics, we reexamine the study of Ripka et al. [26] in detail. Several experimental β-turn structures were extracted from the PDB and compared with BZD conformers. Both experimental β-turns derived from crystal structures of proteins as well as modeled classical β-turn structures were compared with BZD conformers to examine their geometrical basis of β-turn mimicry of β-turns.

## Methods

### Construction of molecular models

All modeling utilized SYBYL 7.1 [28]. Two experimental ring conformers for BZDs were modeled according to the structure shown in Fig. 2A. The modeled structures were fully minimized with the MM3 program included in SYBYL 7.1 using default conditions (Powell minimization, gradient termination = 0.05 kcal/(mol A)). The minimized structures are shown in Fig. 2B,C and the coordinates listed in Tables S1 and S2, respectively. Two other 3-D structures of BZD were modeled according to the diagram shown in Fig. 3D. The difference between structures A and D is the chirality at the ring carbon to which R3 is attached. As with structure 2A, two 3-D representations of chemical structure D were considered and minimized using MM3. The structures are shown in Fig. 3E,F, and the coordinates are listed in Tables S3 and S4, respectively. To model various classical β-turn structures, tetraalanine peptides were generated using SYBYL 7.1, and torsion angles of the backbone set to

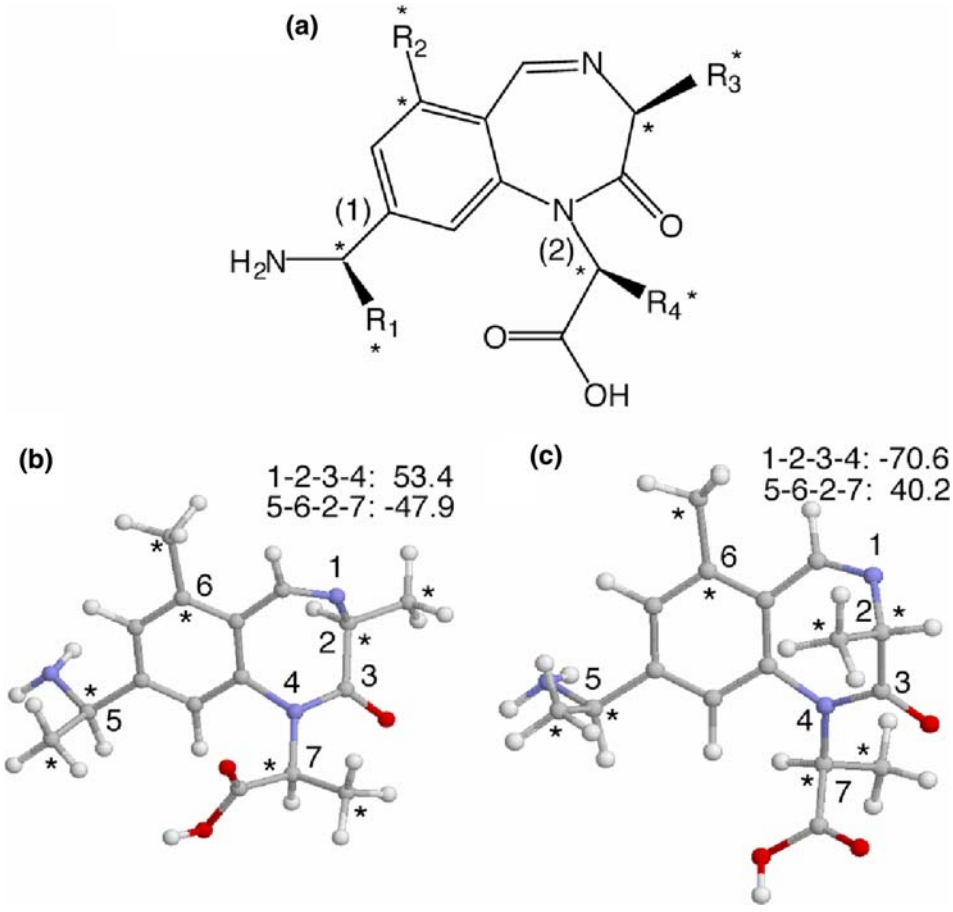


**Fig. 2** (**A**) Chemical structure of BZD. 3-D structures (**B**) and (**C**) corresponding to minimized structure (**A**). Atoms shown by asterisks are used for comparison. The units of 1-2-3-4 and 5-6-2-7 are torsional degrees

those associated with the different classes (I, I′, II, II′, III and VI) of $\beta$-turn types (Table 1).

Ripka et al. established a limited basis set of various types of experimental reverse turns from X-ray structures of proteins available from the PDB [27] to compare with BZD conformers [26] as shown in Table 2 of their paper. They failed, however, to include the necessary PDB accession numbers for clear identification of the X-ray structure utilized. A similar set of turns from crystal structures that corresponded to the basis set were identified from the PDB using the keywords shown in Table 3. About 10–40 potential reverse turns for each type of PDB structures that had been deposited in 1993 or before were selected based on the date of Ripka's publication [26]. From these crystal structures, the corresponding turn sequences shown in Table 2 were extracted. $\phi$, $\Psi$ and $\omega$ angles of residues i+1 and i+2 of the extracted turns were measured to compare with those of classical $\beta$-turns. The RMSD values from a comparison of modeled classical turns with the experimental $\beta$-turn structures were calculated, and the pair of turns that yielded the smallest RMSD value was defined as ''The Closest'' experimental $\beta$-turn to classical $\beta$-turn.

## Computational details

First, conformers of BZDs and classical reverse turns were generated using the ''Systematic Search'' module in SYBYL 7.1. All hydrogen atoms were omitted from those molecules to simplify computations and avoid degrees of freedom to spin methyl rotors. The $C_\alpha$–CO bond ($\Psi$) of residue i and N–$C_\alpha$ bond ($\Phi$) of residue i+3 of each peptide turn (Fig. 1) were rotated, while $\Psi$, $\Phi$ of residues i+1 and i+2 were constrained to values corresponding to classical reverse-turn types, to generate conformers with specific orientations of the four side chains under consideration. Bonds (1) and (2) of BZD shown in Fig. 2A or 3D were rotated to explore orientations of comparable vectors. Bonds of BZD selected corresponded to those of the $C_\alpha$–CO bond of residue i and N–$C_\alpha$ bond of residue i+3 of a peptide. The van der Waals Radius Scale Factors were set to 0.90, 0.87 and 0.75 for General, 1–4 and H-Bonds, respectively [29]. The rotational increment chosen was 1°, generating a theoretically number of possible conformers of 129,600. Because of steric exclusion due to VDW overlap of many conformers, however, the allowed number of conformers was significantly

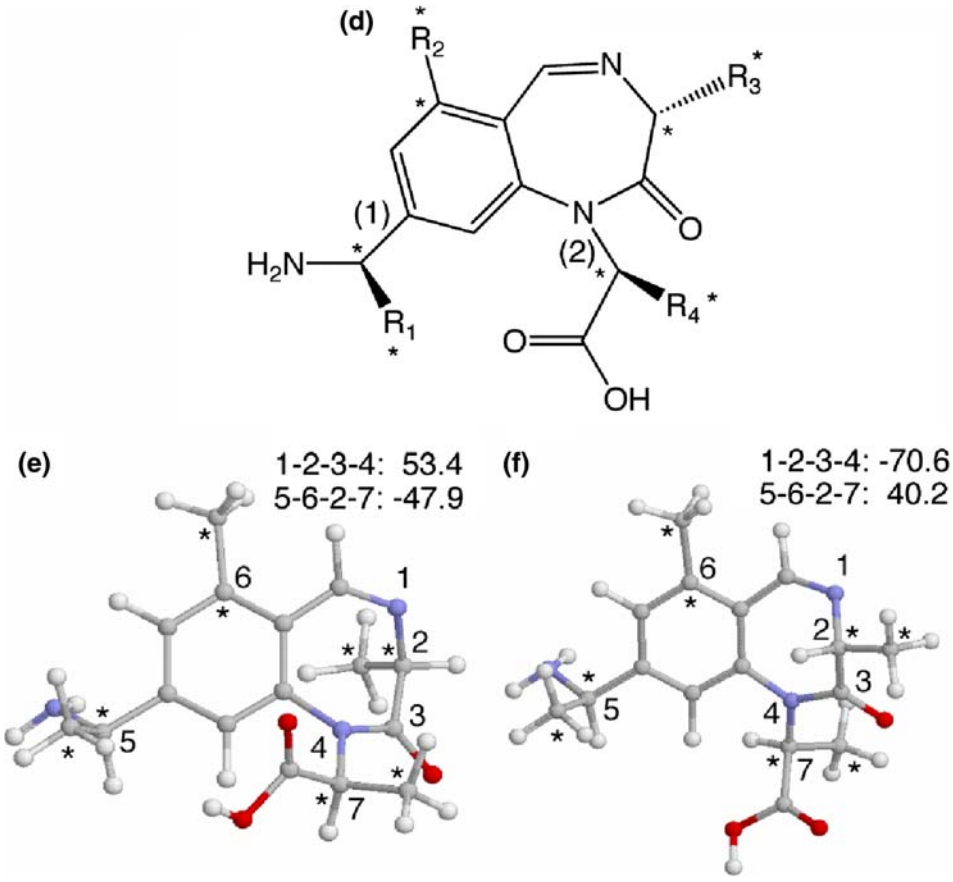


**Fig. 3** (**D**) Chemical structure of $R_3$-chiral alternative BZD. 3-D structures (**E**) and (**F**) corresponding to minimized structure (**D**). Atoms shown by asterisks are used for comparison. The units of 1-2-3-4 and 5-6-2-7 are torsional degrees

decreased to those shown in Table 4. For the experimental $\beta$-turns, only one conformer of a turn obtained from the original crystal data was used.

All the effective conformers of BZD were fit to those of the experimental $\beta$-turns or models of classical $\beta$-turns. As with Ripka's study [26], an RMSD calculation was made for each overlap of the four side-chain vectors. Since a huge number of conformations for comparison were generated, a program for rapid comparison of the two structures and computation of the RMSD values was required. The algorithm of the program follows the ''Fit Atoms'' module of SYBYL 7.1. The least RMSD value was selected for each comparison of a BZD conformer with a reverse turn (either experimental or classical), and the results are shown in Tables S5 to S11.

**Table 3** Search result from the PDB

| Type | Keyword | Hits | Selected[a] |
|---|---|---|---|
| Type I | Subtilisin | 168 | 15 |
| Type I′ | Staphylococcal Nuclease | 67 | 8 |
| Type II | Lysozyme | 932 | 34 (38)[b] |
| Type II′ | Carboxypeptidase | 154 | 10 |
| Type III | Myoglobin | 228 | 35 |
| Type IV | Chymotrypsin | 413 | 7 (10)[b] |
| Type VI | Ribonuclease | 553 | 10 |

[a] Deposited in 1993 or before

[b] Some PDB files have two structures. Numerals in parenthesis are number of structures used in this study

## Results

Table 5 shows the summary of the RMSD calculations. Three kinds of numbers are shown for each $\beta$-turn type: i.e., the upper is ''Experimental Turn'', the middle is ''The Closest'' and the lower is ''Ideal Turn''. The row, ''Experimental Turn'', shows the least RMSD value of all the BZD conformers compared to the experimental $\beta$-turn. The row, ''The Closest'', shows the least RMSD value of the experimental $\beta$-turn selected for the ''Experimental Turn'' comparison to models of the classical $\beta$-turn. The row, ''Ideal Turn'', shows the least RMSD value of the BZD conformers compared to models of the classical $\beta$-turn. PDB entry codes are also shown in the rows of ''Experimental Turn'' and ''The Closest''. $\phi_{i+1}$, $\Psi_{i+1}$, $\phi_{i+2}$, and $\Psi_{i+2}$ angles of those structures are shown in Table 1. All angles satisfy the distance criteria for $\beta$-turns by Hutchinson et al. [30].

**Table 4** The number of conformers of BZDs and the classical $\beta$-turns used in this study

| BZD Structure[a] | Conformer | $\beta$-Turn | Conformer |
|---|---|---|---|
| (b) | 26280 | Type I | 33,420 |
| (c) | 19440 | Type I′ | 31,443 |
| (e) | 26280 | Type II | 29,963 |
| (f) | 19440 | Type II′ | 31,813 |
| | | Type III | 38,192 |
| | | Type VI | 10,602 |

[a] Corresponds to Figs. 2, 3

When comparing columns (B) and (C) in Table 5, the three RMSD values for structure B are smaller than those for structure C for reverse-turn Types I′ and II′. The values of ''Experimental Turn'' and ''The Closest'' for structure B are the same as those for structure C, but are slightly smaller than those for structure C in Table S8. On the other hand, the three values for structure C are smaller than those for structure B for reverse-turn Types I, II, III and IV. In Type VI, ''Experimental Turn'' and ''The Closest'' for structure C are smaller than those for structure B, while Ideal Turn for structure B is smaller than that for structure C. In addition, structure E and structure F in Table 5 were also compared. The three RMSD values for structure E are smaller than those for structure F except reverse-turn Type I′.

Both structures A and D have two RMSD values for the overlap with each $\beta$-turn type. The smallest value of the two was defined as the least RMSD value for structures A or D, and these values are shown in Table 6. All the RMSD values were significantly small, less than 1 Å. These results are discussed in the next section.

## Discussion

### Comparison with Ripka's RMSD values

Ripka et al. explored $\beta$-turn peptidomimetics design, starting from the Type I turn [26]. After several iterations, they selected the BZD scaffold as a possible reverse-turn peptidomimetic. They compared molecular mechanics (MM) structures of BZDs with $\beta$-turn structures from protein crystal structures shown in Table 2 and found that, in addition to Type I, other turns (Types I′, II, II′, III, IV and VI) fit the BZD structures.

Their RMSD values [26] are shown in the rightmost column of Tables 5 and 6. All the values were less than 1 Å (0.26–0.79 Å). From such good agreement, Ripka et al. argued that the BZD nucleus provided an excellent potential mimic for all $\beta$-turn types examined. As mentioned in the Results section, our RMSD values were also less than 1 Å, although we were not sure which PDB structures corresponding to those of Ripka et al. [26] should be utilized for direct comparison. When their RMSD values were compared with our RMSD values for the overlap of ''Experimental Turn'' and structure A, Types I′, II and III (0.55, 0.48 and 0.55 Å) were smaller than their values (0.65, 0.59 and 0.79 Å), but the differences were less than ca. 0.2 Å, in most cases (Table 6). However, the difference for Types II′ and VI were larger, ca. 0.4 and 0.5 Å, respectively. We assumed that these differences occurred because the exact PDB entries used were not equivalent to the original coordinates generating Ripka's results [26].

Although Ripka et al. [26] used structure A (Fig. 2) in their paper [26], its enantiomer, the chiral structure D (Fig. 3), was also considered in this study because it was readily accessible synthetically and available in the Cambridge Structural Database [31] as MIGBEJ [32]. Other BZD-like structures available were QIBLIW [33], SEYRIX01 [34] and YACGOY [34]. The least RMSD values for the overlap of the ''Experimental Turn'' and structure D are also significantly small, 0.48–0.75 Å (Table 6). The RMSD values for Types I′ (0.55 Å), II (0.48 Å) and III (0.75 Å) were smaller than Ripka's results, but all the differences were within ca. 0.2 Å. Structure D fitted the experimental $\beta$-turn better than structure A, except Types I′, II and III. The RMSD values for the experimental turns of Types I′ and II were the same between structure A and D because a glycine residue was found in i+2 position; thus, peptides have no $\alpha$–$\beta$ vector at i+2 position. As in other similar cases, atoms e and e′ (Fig. 1) were used for the overlaps. However, atom e of structures B and E (or C and F) shared the same positions with each other (Figs. 2, 3). For this reason, the RMSD values did not change, regardless of the direction of R3. However, the RMSD values for the overlap of the ideal turns of Types I′ and II and structures (a) and (d) were also small (0.66–0.81 Å). Even if the i+2 C–C vector existed, Types I′ and II would still give small RMSD values. Types I and II′ turns also give small RMSD values with or without a glycine residue (Tables 2 and 6). Our results both reproduce and extend those of Ripka et al. as they show that both chiral molecules A and D and their ring conformers are necessary to mimic the full sets of $\beta$-turn structures with precision.

**Table 5** The least RMSD values obtained by the overlaps of BZDs and various $\beta$-turns

| Structure | RMSD (Å) | | | | Ripka[a] (Å) |
|---|---|---|---|---|---|
| | (a) | | (d) | | |
| | (b) | (c) | (e) | (f) | |
| *Type I* | | | | | |
| "Experimental Turn" (PDB)[b] | 1.47 (1SBT) | 0.65 (1SBT) | 1.68 (1SBT) | 0.60 (1SBT) | 0.56 |
| "The Closest" (1SBT) | 1.47 | 0.65 | 1.68 | 0.60 | |
| Ideal Turn | 1.58 | 0.48 | 1.70 | 0.69 | |
| *Type I′* | | | | | |
| "Experimental Turn" (PDB)[b] | 0.55 (2SNM) | 1.52 (1STN) | 0.55 (2SNM) | 1.52 (1STN) | 0.65 |
| "The Closest" (2SNS) | 0.58 | 1.63 | 0.58 | 1.63 | |
| Ideal Turn | 0.66 | 1.55 | 0.81 | 1.45 | |
| *Type II* | | | | | |
| "Experimental Turn" (PDB)[b] | 0.68 (7LYZ) | 0.48 (132L) | 0.68 (7LYZ) | 0.48 (132L) | 0.59 |
| "The Closest" (1LMA) | 0.77 | 0.69 | 0.77 | 0.69 | |
| Ideal Turn | 1.01 | 0.78 | 1.16 | 0.74 | |
| *Type II′* | | | | | |
| "Experimental Turn" (PDB)[b] | 0.86 (1CPS) | 0.86 (4CPA) | 1.16 (6CPA) | 0.56 (4CPA) | 0.47 |
| "The Closest" (1CBX) | 0.91 | 0.91 | 1.22 | 0.67 | |
| Ideal Turn | 0.85 | 1.11 | 1.10 | 0.94 | |
| *Type III* | | | | | |
| "Experimental Turn" (PDB)[b] | 1.69 (2MGL) | 0.55 (2CMM) | 1.77 (2MGL) | 0.75 (2CMM) | 0.79 |
| "The Closest" (1MBC) | 1.81 | 0.69 | 1.88 | 0.92 | |
| Ideal Turn | 1.89 | 0.60 | 1.94 | 0.90 | |
| *Type IV* | | | | | |
| "Experimental Turn" (PDB)[b] | 1.21 (1ACB) | 0.74 (5CHAb[c]) | 1.42 (1CHO) | 0.69 (1ACB) | 0.54 |
| "The Closest" | n/a | n/a | n/a | n/a | |
| Ideal Turn | n/a | n/a | n/a | n/a | |
| *Type VI* | | | | | |
| "Experimental Turn" (PDB)[b] | 1.26 (1RBG) | 0.76 (1RBD) | 1.45 (1RBG) | 0.50 (1RNV) | 0.26 |
| "The Closest" (1RBF) | 1.33 | 0.80 | 1.50 | 0.60 | |
| Ideal Turn | 0.80 | 1.04 | 1.04 | 0.82 | |

[a] Ref. 26

[b] PDB entry code of the structure that gives the RMSD value

[c] Structure B in 5CHA

## Mimicking the $\beta$-turn

When making comparisons between BZD conformers and those of reverse turns, four data sets were considered; the BZD set of conformers, the ideal $\beta$-turn (four torsional angles of backbone constrained) set of conformers, the experimental set from Ripka-selected crystal structures, and the "Closest" set. When RMSD values for "The Closest" were compared with those for the "Experimental Turn" for each $\beta$-turn type with each structure, the values of "The Closest" were larger than those of the "Experimental Turn" except for Type I (Tables 5 and 6). In case of Type I, $\phi$ and $\Psi$ angles of all peptides, except 1SBT, were Type II (Type IV for 2SBT) [30] rather than Type I (Table 7). For this reason, all results but 1SBT were excluded and consequently, the values for Type I "Experimental Turn" correspond to those for "The Closest". The result shows that the experimental $\beta$-turn structure that gave the least RMSD value does not necessarily correspond to "The Closest" experimental $\beta$-turn structure to the ideal $\beta$-turn. We compared BZDs with modeled classical $\beta$-turns, as well. Regarding structure A, the RMSD values for classical $\beta$-turns were larger than those for the experimental $\beta$-turns except Types I (classical: 0.48 Å, experimental: 0.65 Å) and II′ (classical: 0.85 Å, experimental: 0.86 Å) (Table 6). For structure D, all classical $\beta$-turn RMSDs were larger than those for "Experimental Turn"s (Table 6). This result suggests that experimental $\beta$-turns fits the BZD scaffold better than classical $\beta$-turns. However, not all the experimental $\beta$-turns fit the BZD scaffold better. In case of structure A, the RMSD values for classical $\beta$-turn of Types I, II′ and III (0.48, 0.85 and 0.60 Å) are smaller than those for "The Closest" (0.65, 0.91 and 0.69 Å), and in structure D, the RMSD for the Type III

**Table 6** The least RMSD values obtained by the overlaps of BZDs with various $\beta$-turns

| Structure | (a) | | (d) | | Ripka[a] (Å) |
|---|---|---|---|---|---|
| | Origin | RMSD (Å) | Origin | RMSD (Å) | |
| *Type I* | | | | | |
| "Experimental Turn" (PDB)[b] | (c) | 0.65 (1SBT) | (f) | 0.60 (1SBT) | 0.56 |
| "The Closest" (1SBT) | (c) | 0.65 | (f) | 0.60 | |
| Ideal Turn | (c) | 0.48 | (f) | 0.69 | |
| *Type I′* | | | | | |
| "Experimental Turn" (PDB)[b] | (b) | 0.55 (2SNM) | (e) | 0.55 (2SNM) | 0.65 |
| "The Closest" (2SNS) | (b) | 0.58 | (e) | 0.58 | |
| Ideal Turn | (b) | 0.66 | (e) | 0.81 | |
| *Type II* | | | | | |
| "Experimental Turn" (PDB)[b] | (c) | 0.48 (132L) | (f) | 0.48 (132L) | 0.59 |
| "The Closest" (1LMA) | (c) | 0.69 | (f) | 0.69 | |
| Ideal Turn | (c) | 0.78 | (f) | 0.74 | |
| *Type II′* | | | | | |
| "Experimental Turn" (PDB)[b] | (b) | 0.86 (1CPS) | (f) | 0.56 (4CPA) | 0.47 |
| "The Closest" (1CBX) | (b) | 0.91 | (f) | 0.67 | |
| Ideal Turn | (b) | 0.85 | (f) | 0.94 | |
| *Type III* | | | | | |
| "Experimental Turn" (PDB)[b] | (c) | 0.55 (2CMM) | (f) | 0.75 (2CMM) | 0.79 |
| "The Closest" (1MBC) | (c) | 0.69 | (f) | 0.92 | |
| Ideal Turn | (c) | 0.60 | (f) | 0.90 | |
| *Type IV* | | | | | |
| "Experimental Turn" (PDB)[b] | (c) | 0.74 (5CHAb[c]) | (f) | 0.69 (1ACB) | 0.54 |
| "The Closest" | | n/a | | n/a | |
| Ideal Turn | | n/a | | n/a | |
| *Type VI* | | | | | |
| "Experimental Turn" (PDB)[b] | (c) | 0.76 (1RBD) | (f) | 0.50 (1RNV) | 0.26 |
| "The Closest" (1RBF) | (c) | 0.80 | (f) | 0.60 | |
| Ideal Turn | (b) | 0.80 | (f) | 0.82 | |

[a] Ref. 26

[b] PDB entry code of the structure that gives the RMSD value

[c] Structure B in 5CHA

turn is smaller ("Classical Turn": 0.90 Å, "The Closest": 0.92 Å). Therefore, the experimental $\beta$-turns included in the basis set do not always give lower RMSD values as some of the classic $\beta$-turns gives a lower RMSD value for some turn types.

## Why does the BZD scaffold mimic $\beta$-turns?

The rightmost column of Table 1 shows $C_{\alpha I}$–$C_{\alpha i+1}$–$C_{\alpha i+2}$–$C_{\alpha i+3}$ dihedral angles of $\beta$-turn structures. A $\beta$-turn causes a reverse turn in the peptide chain, and consequently, the dihedral angles should be between –90 and 90°. All experimental dihedral values of reverse turns examined satisfied this criterion. The corresponding dihedral angles of BZD were –47.9, 40.2, –47.9 and 40.2° for structures B, C, E and F, respectively, and were within this range. Therefore, the BZD scaffold incorporates a geometrical moiety analogous to a reverse turn within its chemical structure.

The distances between $C_\alpha$ atoms were measured and shown in Table 8. $C_{\alpha I}$–$C_{\alpha i+1}$, $C_{\alpha i+1}$–$C_{\alpha i+2}$, $C_{\alpha i+2}$–$C_{\alpha i+3}$ and $C_{\alpha I}$–$C_{\alpha i+3}$ distances of BZD were 3.73, 4.02 (or 4.06), 3.84 and 5.07 (or 5.95) Å, respectively. These distances were similar to most of the corresponding distances of both experimental and classical $\beta$-turns; i.e., $C_{\alpha I}$–$C_{\alpha i+1}$: 3.70–3.91 Å, $C_{\alpha i+1}$–$C_{\alpha i+2}$: 2.80–3.90 Å, $C_{\alpha i+2}$–$C_{\alpha i+3}$: 3.75–3.90 Å and $C_{\alpha I}$–$C_{\alpha i+3}$: 4.08–6.01 Å. If this similarity determined the good fit between BZD and $\beta$-turns, all BZD structures would fit $\beta$-turns. However, only structures C and F fit most types of $\beta$-turn (Table 6). In the "Experimental Turn"s of Type II′, structure B fit better, but the difference of RMSD values from structure C only varied slightly (Tables 5 and S8). However, structures C and F did not fit the Type I′ turns (Table 5); Type I′ fit structures B and E well. This is because the dihedral angle $\theta$ of Type I′ and the corresponding dihedral angle of structures B and E are similar, but much different from the other structures. The angles are shown in Figs. 2, 3 and Table 1. The dihedral angles $\theta$ of Type I′ were –47.3 to –51.8°, which was similar to that of structures B and E (–47.9°). One can see that structures B and E fit the experimental Type I′ turns better than structure C and F (Fig. 4). The two observed conformers of the central ring structure of BZD were required to facilitate the fits to all types of $\beta$-turn.

**Table 7** $\phi$ and $\Psi$ angles (degrees) of residues i+1 and i+2 of selected experimental Type I and ideal Types I and II

| Structure | i+1 | | i+2 | |
|---|---|---|---|---|
| | $\phi$ | $\Psi$ | $\phi$ | $\Psi$ |
| Type I (ideal) | –60.0 | –30.0 | –90.0 | 0.0 |
| 1SBT | –52.3 | –58.2 | –90.8 | 22.0 |
| Type II (ideal) | –60.0 | 120.0 | 80.0 | 0.0 |
| 1S01 | –53.7 | 136.9 | 71.3 | 7.1 |
| 1S02 | –62.9 | 138.9 | 69.3 | 15.9 |
| 1SBN | –58.1 | 134.7 | 70.2 | –10.4 |
| 1SIB | –65.3 | 136.0 | 82.8 | –6.7 |
| 1ST2 | –49.2 | 132.3 | 73.0 | 5.8 |
| 1SUB | –54.2 | 137.9 | 70.9 | 6.3 |
| 1SUC | –66.2 | 134.0 | 72.2 | 16.2 |
| 1SUD | –60.2 | 130.4 | 77.1 | 10.4 |
| 2SBT | –81.9 | 126.5 | 126.9 | –41.0 |
| 2SIC | –51.8 | 128.0 | 76.7 | 8.2 |
| 2SNI | –59.7 | 137.0 | 64.7 | 21.2 |
| 2ST1 | –54.0 | 136.7 | 70.3 | 6.9 |
| 3SIC | –62.5 | 139.6 | 65.6 | 7.9 |
| 5SIC | –60.6 | 147.4 | 65.7 | 1.4 |

**Table 8** $C_\alpha$–$C_\alpha$ distance (Å) of BZDs and $\beta$-turn structures

| Structure | $C_{\alpha I}$–$C_{\alpha i+1}$ | $C_{\alpha i+1}$–$C_{\alpha i+2}$ | $C_{\alpha i+2}$–$C_{\alpha i+3}$ | $C_{\alpha i+3}$–$C_\alpha$ |
|---|---|---|---|---|
| BZD (b) | 3.73 | 4.02 | 3.84 | 5.07 |
| BZD (c) | 3.73 | 4.06 | 3.84 | 4.95 |
| BZD (e) | 3.73 | 4.02 | 3.84 | 5.07 |
| BZD (f) | 3.73 | 4.06 | 3.84 | 4.95 |
| Type I (1SBT) | 3.91 | 3.82 | 3.90 | 4.97 |
| Type I (Ideal) | 3.82 | 3.82 | 3.82 | 4.64 |
| Type I′ (1STN) | 3.83 | 3.78 | 3.85 | 5.19 |
| Type I′ (2SNM) | 3.79 | 3.76 | 3.80 | 5.06 |
| Type I′ (2SNS) | 3.79 | 3.80 | 3.80 | 4.87 |
| Type I′ (Ideal) | 3.82 | 3.82 | 3.82 | 4.64 |
| Type II (132L) | 3.75 | 3.78 | 3.80 | 5.69 |
| Type II (1LMA) | 3.77 | 3.79 | 3.82 | 5.59 |
| Type II (7LYZ) | 3.81 | 3.82 | 3.79 | 5.45 |
| Type II (Ideal) | 3.82 | 3.82 | 3.82 | 4.65 |
| Type II′ (1CBX) | 3.85 | 3.90 | 3.80 | 5.09 |
| Type II′ (1CPS) | 3.80 | 3.80 | 3.80 | 5.06 |
| Type II′ (4CPA) | 3.86 | 3.87 | 3.80 | 5.19 |
| Type II′ (6CPA) | 3.83 | 3.80 | 3.76 | 5.21 |
| Type II′ (Ideal) | 3.82 | 3.82 | 3.82 | 4.65 |
| Type III (1MBC) | 3.77 | 3.79 | 3.82 | 5.86 |
| Type III (2CMM) | 3.80 | 3.84 | 3.75 | 5.28 |
| Type III (2MGL) | 3.70 | 3.82 | 3.84 | 5.69 |
| Type III (Ideal) | 3.82 | 3.82 | 3.82 | 5.37 |
| Type IV (1ACB) | 3.74 | 3.81 | 3.76 | 6.01 |
| Type IV (1CHO) | 3.82 | 3.83 | 3.83 | 5.91 |
| Type IV (5CHAb) | 3.86 | 3.84 | 3.78 | 5.88 |
| Type VI (1RBD) | 3.85 | 2.95 | 3.81 | 5.62 |
| Type VI (1RBF) | 3.81 | 2.90 | 3.82 | 5.62 |
| Type VI (1RBG) | 3.84 | 2.96 | 3.81 | 5.35 |
| Type VI (1RNV) | 3.86 | 2.98 | 3.76 | 5.35 |
| Type VI (Ideal) | 3.82 | 2.80 | 3.82 | 4.08 |

## Comparison of BZD with a new classification of reverse turns

Tran et al. suggested a new classification of reverse turns determined by the orientation of the four side-chains on residues i through i+3 [35]. There are nine classes of reverse turns with nearly identical side-chain orientations found in their clustering scheme with approximately 90% of $\beta$-turns found in the PDB belongs to one of the nine classes, whereas only 57–68% of $\beta$-turns are classified into the eight different classical backbone families (Types I, II, I′, II′, VIII, VIa1, VIa2 and VIb). The mean structures of each class of Tran et al. [35] were also compared with BZD structures and the results are shown in Table 9. Structures C and F fit every cluster except Cluster 9, whereas structures B and E fit only Cluster 9. The reason was the same as the case of Type I′ and structure B or E. The dihedral angle $\theta$ of Cluster 9 (–41.5°) is close to the corresponding dihedral angle of structures B and E (–47.9°) rather than those of structures C

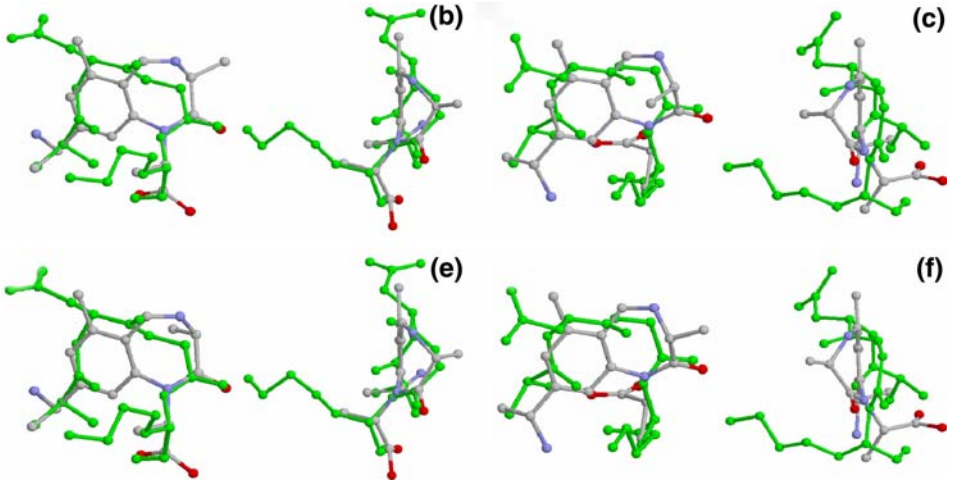


**Fig. 4** Orthogonal views of overlaps of Ala94-Lys97 of 2SNM.pdb (green) and structures (**B**) and (**E**) and Ala94-Lys97 of 1STN.pdb (green) and structures (**C**) and (**F**) (Figs. 2, 3). These give the least RMSD values shown in Table 5

**Table 9** The least RMSD values obtained by the overlap of BZDs, and the mean structures of the clusters in the new classification of $\beta$-turns (Tran et al.)

| Mean structure | $\theta^a$ (degree) | RMSD (Å) | | | |
|---|---|---|---|---|---|
| | | (a) | | (d) | |
| | | (b) | (c) | (e) | (f) |
| Cluster 1 | 57.6 | 1.96 | 0.65 | 1.99 | 0.89 |
| Cluster 2 | 24.5 | 1.44 | 0.59 | 1.52 | 0.67 |
| Cluster 3 | 31.3 | 1.51 | 0.76 | 1.57 | 0.88 |
| Cluster 4 | 5.9 | 1.08 | 0.83 | 1.25 | 0.74 |
| Cluster 5 | 50.0 | 1.63 | 0.62 | 1.74 | 0.74 |
| Cluster 6 | 56.6 | 2.07 | 0.55 | 2.06 | 0.83 |
| Cluster 7 | 9.0 | 1.08 | 0.76 | 1.26 | 0.68 |
| Cluster 8 | 31.8 | 1.51 | 0.75 | 1.59 | 0.78 |
| Cluster 9 | –41.5 | 0.62 | 1.60 | 0.82 | 1.47 |

[a] $C_{\alpha I}$–$C_{\alpha i+1}$–$C_{\alpha i+2}$–$C_{\alpha i+3}$ of the clusters

and F (40.2°). Figure 5 shows the overlaps of Cluster 9 and BZDs that give the lowest RMSD values. One can see that structures C and F did not fit Cluster 9 of Tran et al. [35] well.

Both structures A and D had two RMSD values for the overlap with each cluster based on the two ring conformers. When the smallest value of the two was defined as the least RMSD value for structure A or D, all the RMSD values were significantly small (structure A: 0.55–0.83 Å and structure D: 0.67–0.89 Å). It is highly significant that the BZD scaffold can mimic reverse turns, whether the orientation of the four side chains of the reverse turn are the direct basis for comparison, or with an abstraction based on averaging the turns in the entire PDB as with the methodology of Tran et al. [35]. Since side-chain interactions are a predominate motif for turn recognition in biological systems, this analysis of the ability of benzodiazepines to mimic reverse turns underscores the experimental results from high-thoughput screens of benzodiazepines against a variety of receptors.

## Conclusion

We reexamined the hypothesis that the benzodiazepine scaffold can mimic the set of reverse turn structures seen in proteins and obtained small RMSD values (less than 1 Å) for the overlap of BZD substituents (requiring inclusion of both chirality and ring conformations) with every class of reverse turn (whether modeled from classical turns or as observed experimentally). These results confirmed and extended those of Ripka et al. When comparing the fit of BZD to experimental or modeled classic $\beta$-turn, experimental $\beta$-turns fit the BZD scaffold better than classical $\beta$-turns, but not all experimental $\beta$-turns fit the BZD scaffold better. BZD mimicked some of the experimental $\beta$-turn structures better than models of classic $\beta$-turns. BZD serves as an excellent privileged scaffold for reverse turns as assessed with the new classification of reverse turns by Tran et al. [35] that focuses on side-chain orientations of the four amino acids of the turn. BZD possesses two distinct conformations of its central ring 7-membered structure each of which is similar to different $\beta$-turn structures. This provides a significant reason why the BZD scaffold can mimic all types of $\beta$-turns in their side-chain orientations. It should be emphasized that the energetic cost ($\Delta G$) of assuming a matching conformation was not considered in these comparisons; rather the sets of sterically allowed conformers were compared to indicate which reverse turns might be mimicked by benzodiazepine scaffolds when bound to a peptide receptor.

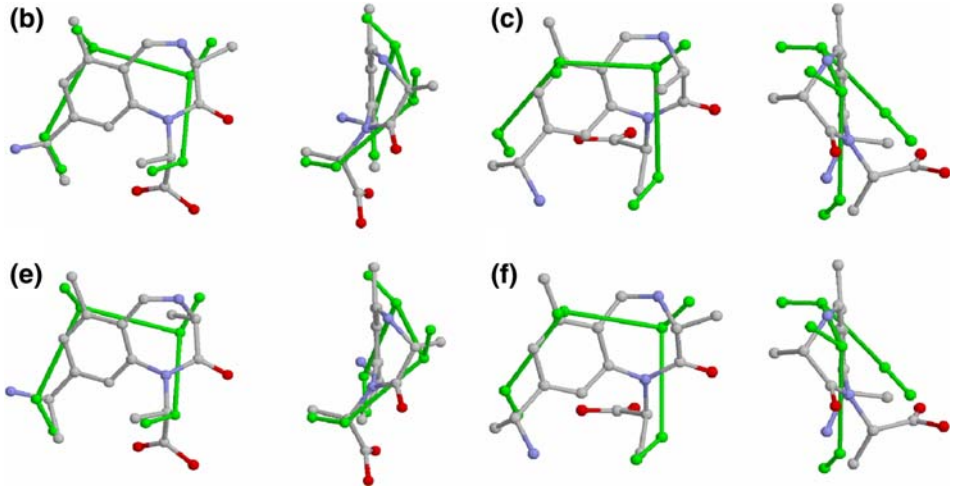


**Fig. 5** Orthogonal views of overlaps of Cluster 9 in the Tran et al. classification of $\beta$-turns (green) and structures (**B**), (**C**), (**E**) and (**F**) (Figs. 2, 3). These give the least RMSD values shown in Table 9

**Acknowledgements** The authors thank Dr. Chris M.W. Ho for programming and optimizing the RMSD fitting program. The authors are also grateful to Dr. Jon Våbenø for meaningful discussion of our preliminary results, and Dr. Christina M. Taylor for reviewing the manuscript. Dr. Masayuki Hata was supported by a grant from the Overseas Advanced Educational Research Practice Support Program by The Ministry of Education, Culture, Sports, Science and Technology (MEXT) of Japan. Research support from the National Institutes of Health (GM068460) is also acknowledged.

## References

1. Rose GD, Gierasch LM, Smith JA (1985) Turns in peptides and proteins. In: Adv Protein Chem, vol 37. Academic Press, pp 1–109
2. Stanfield RL, Fieser TM, Lerner RA, Wilson IA (1990) Science 248(4956):712–719
3. Rini JM, Schulze-Gahmen U, Wilson IA (1992) Science 255(5047):959–965
4. Garcia KC, Ronco PM, Verroust PJ, Brünger AT, Amzel LM (1992) Science 257(5069):502–507
5. Nikiforovich GV, Marshall GR (1993) Biochem Biophys Res Commun 195(1):222–228
6. Plucinska K, Kataoka T, Yodo M, Cody WL, He JX, Humblet C, Lu GH, Lunney E, Major TC, Panek RL, Schelkun P, Skeean R, Marshall GR (1993) J Med Chem 36(13):1902–1913
7. Kyle DJ, Blake PR, Smithwick D, Green LM, Martin JA, Sinsko JA, Summers MF (1993) J Med Chem 36(10):1450–1460
8. Nikiforovich GV, Marshall GR (1993) Int J Peptide Protein Res 42(2):171–180
9. Nikiforovich GV, Marshall GR (1993) Int J Peptide Protein Res 42(2):181–193
10. Reddy DV, Jagannadh B, Dutta AS, Kunwar AC (1995) Int J Peptide Protein Res 46(1):9–17
11. Nutt RF, Veber DF, Saperstein R (1980) J Am Chem Soc 102(21):6539–6545
12. Brady SF, PalevedaJr WJ, Arison BH, Saperstein R, Brady EJ, Raynor K, Reisine T, Veber DF, Freidinger RM (1993) Tetrahedron 49(17):3449
13. Ripka AS, Rich DH (1998) Curr Opin Chem Biol 2(4):441
14. Suat K, Jois SDS (2003) Curr Pharm Des 9(15):1209–1224
15. Hirschmann R, Nicolaou KC, Pietranico S, Leahy EM, Salvino J, Arison B, Cichy MA, Spoors PG, Shakespeare WC, Sprengeler PA, Hamley P, Smith AB III, Reisine T, Raynor K, Maechler L, Donaldson C, Vale W, Freidinger RM, Cascieri MR, Strader CD (1993) J Am Chem Soc 115(26):12550–12568
16. Hirschmann R, Yao W, Cascieri MA, Strader CD, Maechler L, Cichy-Knight MA, Hynes J, van Rijn RD, Sprengeler PA, Smith AB (1996) J Med Chem 39(13):2441–2448
17. Reaka AJH, Ho CMW, Marshall GR (2002) J Comput-Aided Mol Des 16(8–9):585–600
18. Hirschmann R, Sprengeler PA, Kawasaki T, Leahy JW, Shakespeare WC, Smith AB (1992) J Am Chem Soc 114(24):9699–9701
19. Nagai U, Sato K, Nakamura R, Kato R (1993) Tetrahedron 49(17):3577–3592
20. Cornille F, Slomczynska U, Smythe ML, Beusen DD, Moeller KD, Marshall GR (1995) J Am Chem Soc 117(3):909–917
21. Evans BE, Rittle KE, Bock MG, DiPardo RM, Freidinger RM, Whitter WL, Lundell GF, Veber DF, Anderson PS, Chang RSL, Lotti VJ, Cerino DJ, Chen TB, Kling PJ, Kunkel KA, Springer JP, Hirshfield J (1988) J Med Chem 31(12):2235–2246
22. Horton DA, Bourne GT, Smythe ML (2003) Chem Rev 103(3):893–930
23. Breinbauer R, Vetter IR, Waldmann H (2002) Angew Chem Int Ed 41(16):2878–2890
24. Fecik RA, Frank KE, Gentry EJ, Menon SR, Mitscher LA, Telikepalli H (1998) Med Res Rev 18(3):149–185
25. Ellman JA (1996) Acc Chem Res 29(3):132–143
26. Ripka WC, De Lucca GV, Bach AC II, Pottorf RS, Blaney JM (1993) Tetrahedron 49(17):3593–3608
27. Berman HM, Westbrook J, Feng Z, Gilliland G, Bhat TN, Weissig H, Shindyalov IN, Bourne PE (2000) Nucleic Acids Res 28(1):235–242
28. SYBYL 7.1 (2005) Molecular modeling system. Tripos Associates, Inc., St. Louis, MO
29. Iijima H, Dunbar JB Jr, Marshall GR (1987) Proteins 2(4):330–339
30. Hutchinson EG, Thornton JM (1994) Protein Sci 3(12):2207–2216
31. Allen FH (2002) Acta Crystallogr B 58(3–1):380–388
32. Miki T, Kori M, Fujishima A, Mabuchi H, Tozawa R, Nakamura M, Sugiyama Y, Yukimasa H (2002) Bioorg Med Chem 10(2):385–400
33. Visnjevac A, Kojic-Prodic B (2001) Acta Crystallogr E 57(4):o356–o357
34. Rambaud J, Dubourg A, Delarbre J-L, Roger J, Maury L, Declercq J-P (1991) Bull Soc Chim Belg 100(7):521–526
35. Tran T, McKie J, Meutermans W, Bourne G, Andrews P, Smythe M (2005) J Comput-Aided Mol Des 19(8):551–566